

Magnetic Resonance Diffusion Imaging and Micro-CT Imaging of Breast Tumour Microarchitecture

L. J. Friesen Waldner¹, J. A. Kost¹, D. W. Holdsworth¹, B. K. Rutt¹

¹Imaging Research Laboratories, Robarts Research Institute, London, Ontario, Canada

Introduction: The density of microvessels in ‘hotspots’ in the periphery of invasive breast tumours has been shown by histopathology to outperform lymph-node positivity as a predictor for the development of distant metastatic disease [1]. Currently, no non-invasive method of imaging the microvasculature of breast tumours exists. We have developed a magnetic resonance diffusion (MRD) imaging method that allows us to quantitatively measure microvascular flow, which can be modeled as a fast “pseudo-diffusion” process (D3), and two rates of diffusion (slow, D1, and intermediate, D2) of water that are related to tissue microarchitecture in tumours in the mammary fat pads of rats [2]. This study did not compare benign and malignant tumours and considered only the average Ds in a region of interest in the tumour, so heterogeneity, which is known to be diagnostic, was not examined.

Hypothesis: That structures in 3-dimensional (3D) maps of the diffusion parameters of water in tumour tissue correspond to structural differences in the tissue microarchitecture and that maps of the pseudo-diffusion parameters of the microvasculature of a solid breast lesion show microvessel densities and distributions in agreement with values measured by another independent imaging method.

Methods: N-ethyl-N-nitrosourea (ENU) was injected intraperitoneally (180mg/kg body weight) into 30 day old Sprague-Dawley rats [3]. Vascularized mammary tumours developed spontaneously in approximately 90 days. Rats were anaesthetised using ketamine/xylazine. Nineteen tumours were imaged using a 1.5T GE CV/i MRI system, 40mT gradient strength and a quadrature surface RF coil (4cm loops) and the following protocol: single shot SE-EPI, TE/TR=90.1ms/2500ms, FOV=16x8cm, matrix=80x80, slice thickness=5.0mm, 8 averages, 18 b-values (0, 30, 61, 90, 139, 239, 366, 529, 736, 1000, 1500, 2000, 2500, 3000, 3500, 4000, 4500, 5000s/mm²), at each b-value, diffusion encoding was applied along xz, -xz, yz, -yz, xy, -xy directions. Post-mortem, the vasculature of the rats was filled with Microfil MV-122, a radio-opaque contrast agent. Micro-CT images were obtained from the excised tumours using the following protocol: 80kVp, 80µA, 0.5mm aluminium filtration, number of views=720, exposure time/view=1600ms, total acquisition time<2 hours, voxel size=27µm isotropic. Diffusion decay curves (Si/So vs b) were fit on a pixel-by-pixel basis from the MRD images using the non-negative, least squares (NNLS) algorithm. Maps of the three Ds and corresponding fractional volumes contributing to each of the Ds (fs) were generated. Maps of the trace of the tensor were compared to the micro-CT images. Three-dimensional images of the tumour vasculature were constructed from maximum intensity projections of the micro-CT images.

Results: Maps of the diffusion parameters, particularly D2, f1, and f2, show structures that correspond to structures observed in the high resolution STIR images of the tumours. An example of one structured tumour is shown in Fig 1. Micro-CT images (3d projections) of 2 tumours showing differing vascular densities and distributions are shown in Fig 2. Also in Fig 2 are 2d maps of the fast diffusion parameters (D3 and f3) for one slice through the center of the same 2 tumours as the micro-CT images. The average f3's in the whole tumours A and B are 0.04 and 0.10 respectively.

Discussion: The correspondence of structures in some of the diffusion maps to structures observed in the high resolution images suggests that the slow and intermediate diffusion parameters may correlate to tissue microarchitecture. Micro-CT images of the 2 tumours shown in Fig 2 show that A is much less vascular than B. Dark pixels in the D3 maps correspond to very slow or no microvascular flow. Dark pixels in the f3 maps correspond to the absence of or decrease in microvascular volume. Both the D3 and f3 maps of tumour A have a greater number of dark pixels than tumour B suggesting that A is less vascular than B. Further, the average f3 in A (0.04) is less than half that found in B (0.10). This agrees with the micro-CT images. In addition, the micro-CT images show large vessels on the periphery of the tumours and the f3 maps show a corresponding higher concentration of vasculature on the periphery of the tumours.

Conclusions: Maps of the diffusion parameters show structures that agree with structures seen in high resolution MR images of the rat mammary fat pad tumours. Qualitative comparisons of the microvasculature diffusion parameters to micro-CT images of the vasculature show similar densities and distributions of microvessels. Ongoing work involves correlating structures in maps of the slow and intermediate diffusion parameters to tissue microarchitecture as determined by histopathology and correlating the “pseudo-diffusion” rate and fractional volume of the microvascular compartment to similar resolution maps of the micro-CT images and pathologically determined vessel densities and distributions.

Acknowledgements: Financial support from NSERC and the U.S. Army MRMC (DAMD17-01-1-0278).

References:

- 1) DD Dershaw *et al.* Radiology 1987, **164**: 455.
- 2) LJ Friesen Waldner, BK Rutt. Proc. ISMRM (2002) 635.
- 3) G Stoica *et al.* Am J Pathol 1983, **110**:161.

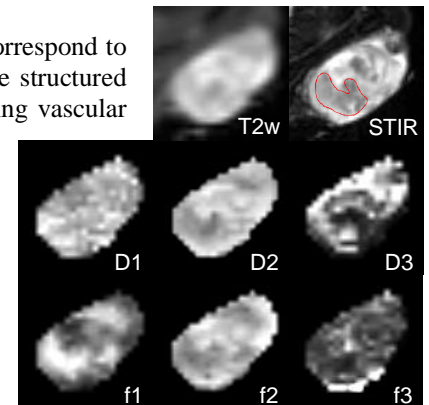


Fig 1: Structures in T2-weighted and STIR images (example ROI in STIR) appear in maps of diffusion parameters (from trace of tensor), particularly in D2, D3, f1, and f2.

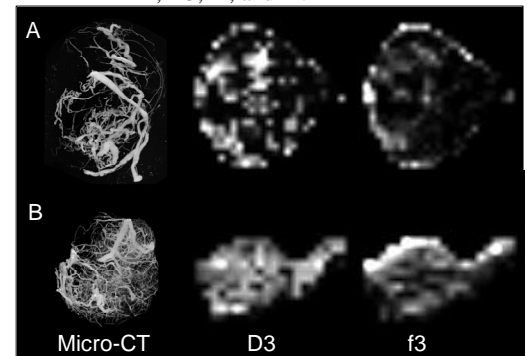


Fig 2: Micro-CT images (maximum intensity projections) of the vasculature of tumours A and B and the corresponding maps of the microvascular diffusion parameters D3 and f3.